Molecular profiling and functional insights of rock bream (Oplegnathus fasciatus) thioredoxin reductase 3-like molecule: Investigation of its transcriptional modulation in response…

Article *in* Gene · June 2015

DOI: 10.1016/j.gene.2015.06.007 · Source: PubMed

CITATION
1

READS
51

3 authors:

Don Anushka Sandaruwan Elvitigala
University of Colombo
63 PUBLICATIONS **240** CITATIONS
SEE PROFILE

Ilson Whang
150 PUBLICATIONS **2,292** CITATIONS
SEE PROFILE

Jehee Lee
Jeju National University
544 PUBLICATIONS **5,282** CITATIONS
SEE PROFILE

Gene 570 (2015) 122–131

Contents lists available at ScienceDirect

Gene

journal homepage: www.elsevier.com/locate/gene

Research paper

Molecular profiling and functional insights of rock bream (*Oplegnathus fasciatus*) thioredoxin reductase 3-like molecule: investigation of its transcriptional modulation in response to live pathogen stress

Don Anushka Sandaruwan Elvitigala [a,b], Ilson Whang [b,*], Jehee Lee [a,b,*]

[a] Department of Marine Life Sciences, School of Marine Biomedical Sciences, Jeju National University, Jeju Self-Governing Province 690-756, Republic of Korea
[b] Fish Vaccine Research Center, Jeju National University, Jeju Self-Governing Province 690-756, Republic of Korea

ARTICLE INFO

Article history:
Received 3 April 2015
Received in revised form 20 May 2015
Accepted 3 June 2015
Available online 6 June 2015

Keywords:
Rock bream
Thioredoxin reductase 3
Genomic organization
Transcriptional modulation
Thiol reductase activity

ABSTRACT

The thioredoxin (Trx) system plays a significant role in cellular antioxidative defense by dismutating the surpluses of reactive oxygen species. Thus, the role of thioredoxin reductase (TrxR) cannot be ignored, owing to its participation in initiating the Trx enzyme cascade. Here, we report the identification and molecular characterization of a teleostean TrxR (RbTrxR-3) ortholog that showed high similarity with the TrxR-3 isoforms of other vertebrates. The complete *RbTrxR-3* coding sequence comprised 1800 nucleotides, encoding a 600-amino acid protein with a predicted molecular mass of ~66 kDa. *RbTrxR-3* consisted of 16 exons separated by 15 introns and had a total length of 12,658 bp. *In silico* analysis of the RbTrxR-3 protein sequence revealed that it possesses typical TrxR domain architecture. Moreover, using multiple sequence alignment and pairwise sequence alignment strategies, we showed that RbTrxR-3 has high overall sequence similarity to other teleostean TrxR-3 proteins, including highly conserved active site residues. Phylogenetic reconstruction of RbTrxR-3 affirmed its close evolutionary relationship with fish TrxR-3 orthologs, as indicated by its clustering pattern. *RbTrxR-3* transcriptional analysis, performed using quantitative polymerase chain reaction (qPCR), showed that *RbTrxR-3* was ubiquitously distributed, with the highest level of mRNA expression in the blood, followed by the gill, and liver. Live bacterial and viral stimuli triggered the modulation of *RbTrxR-3* basal transcription in liver tissues that correlated temporally with that of its putative substrate, rock bream thioredoxin1 under the same conditions of pathogenic stress. Finally, resembling the typical function of TrxR protein, purified recombinant RbTrxR-3 showed detectable dose-dependent thiol reductase activity against 5,5′-dithiobis (2-nitrobenzoic) acid. Taken together, these results suggest that RbTrxR-3 plays a role in the host Trx system under conditions of oxidative and pathogenic stress.

1. Introduction

Mariculture is a branch of aquaculture that is dedicated to the cultivation of edible marine organisms, especially for human consumption. This industry has increased in prominence, owing to the fact that marine organisms are a suitable alternative for current terrestrial resources, and can fulfill the daily nutritional requirements of an ever-increasing global population. In this regard, marine fish cultivation represents a large segment of the mariculture industry, because fish consumption has worldwide popularity. One such delicacy, rock bream (*Oplegnathus fasciatus*), is a cultivable aqua-crop that currently accounts for a considerable proportion of global commercial aquaculture yields, especially in East and South East Asian countries including China, Japan, and Korea. However, marine teleost fish such as rock breams, which are cultivated using intensified technology and under high population densities, are regularly exposed to a wide range of stress factors, most of which can negatively impact on their growth and survival. Pathogenic infections as well as

Abbreviations: Trx, thioredoxin; TrxR, thioredoxin reductase; PCR, polymerase chain reaction; qPCR, quantitative real time PCR; NADPH, nicotinamide adenine dinucleotide phosphate; ROS, reactive oxygen species; NADH, nicotinamide adenine dinucleotide; FAD, flavin adenine dinucleotide; Cys, cysteine; Val, valine; Gly, glycine; Asn, asparagine; bp, base pairs; GS-FLX, genome sequencer-FLX; cDNA, complementary DNA; gDNA, genomic DNA; RNA, ribose nucleic acid; mRNA, messenger ribonucleic acid; BLAST, basic local alignment search tool; SMART, simple modular architecture research tool; ExPASy, Expert Protein Analysis System; MEGA, molecular evolutionary genetics analysis software; BAC, bacterial artificial chromosome; NCBI, National Center for Biotechnology Information; PBS, phosphate buffered saline; OD, optical density; IPTG, isopropyl-β-thiogalactopyranoside; DTNB, 5, 5′-dithiobis (2-nitrobenzoic) acid; SECIS, selenocysteine insertion sequence; MBP, maltose binding protein; RBIV, rock bream irodovirus; NF-κB, nuclear factor κB; SDS-PAGE, sodium dodecyl sulfate polyacrylamide gel electrophoresis; p.i., post injection; SD, standard deviation; UTR, untranslated region; μl, microliter; dNTPs, deoxynucleotide triphosphates; °C, degrees of Celsius; ng, nanogram; rpm, revolutions per minute; h, hours; kDa, kilodalton.

* Corresponding authors at: Marine Molecular Genetics Lab, Department of Marine Life Sciences, College of Ocean Science, Jeju National University, 66 Jejudaehakno, Ara-Dong, Jeju 690-756, Republic of Korea.
E-mail addresses: ilsonwhang@hanmail.net (I. Whang), jehee@jejunu.ac.kr (J. Lee).

http://dx.doi.org/10.1016/j.gene.2015.06.007
0378-1119/

environmental perturbations such as temperature fluctuations, xenobiotics, and hypoxic or hyperoxic conditions may have severe consequences, as these are the main factors responsible for inducing oxidative stress in these animals (Mohapatra et al., 2013). Thus, investigation of naturally existing antioxidative defense mechanisms, especially those elicited under conditions of pathogenic stress in aquacultured fish species like rock bream, is required for the development of a stress-free, sustainable, fish-based aquaculture industry aimed at achieving high productivity.

The cellular antioxidative defense system plays a key role in maintaining redox balance in organisms and preventing oxidative stress by reducing excessive production of reactive oxygen species (ROS), such as peroxides, superoxides, and hydroxyl radicals, which is triggered as a primary host immune defense mechanism against pathogen invasion (Nordberg and Arner, 2001). Endogenous antioxidants including superoxide dismutase, catalase, glutathione, thioredoxin, and glutathione peroxidase play prominent roles in this process, participating in different mechanisms that reduce ROS surpluses. Among these protective mechanisms, the thioredoxin system, which includes nicotinamide adenine dinucleotide phosphate (NADP), thioredoxin reductase (TrxR), and thioredoxin (Trx) as its molecular components, has an indispensable role in controlling oxidative stress and regulating apoptosis (Lu and Holmgren, 2012).

Trx proteins are known to be involved in a wide range of functions in their reduced forms. They provide reducing equivalents to enzymes such as ribonucleotide reductase (Laurent et al., 2013) and thioredoxin peroxidase (Chae et al., 1994), facilitating DNA synthesis and antioxidant defense by reducing ribonucleotides to deoxyribonucleotides and breaking down hydrogen peroxide, respectively. Moreover, extracellular Trx proteins and the truncated form Trx80 were found to participate in inflammatory responses by acting as cytokines and co-cytokines (Nordberg and Arner, 2001). In addition, cell growth induction (Gasdaska and Powis, 1995) and apoptosis inhibition (Baker et al., 1997) are two subsidiary functions of reduced Trx proteins. However, in order to perform these vital functions, oxidized Trx must be reduced by TrxR-mediated catalysis in the presence of NADH or NADPH as an electron donor. To date, TrxR is the only known enzyme that can reduce Trx proteins, reinforcing its essential role in the thioredoxin system.

TrxRs belong to the flavoprotein family of pyridine nucleotide-disulfide oxidoreductases, which also includes several enzymes involved in cellular oxidation and reduction, such as lipoamide dehydrogenase, glutathione reductase, and mercuric ion reductase (Mustacich and Powis, 2000). Members of this family are homodimeric proteins formed from monomers that each contains a flavin adenine dinucleotide (FAD) prosthetic group, an NADPH-binding site, and a redox-active disulfide located in the active site. In addition to Trx, TrxR can act upon other substrates including lipoic acid (Nordberg et al., 1996), lipid hydroperoxides (Bjornstedt et al., 1995), NK-lysin (Andersson et al., 1996), vitamin K_3 (Holmgren, 1979), dehydroascorbic acid (May et al., 1997), ascorbyl free radical (May et al., 1998), and tumor suppressor protein p53 (Casso and Beach, 1996). In the case of NK-lysin, a prominent antibacterial cytotoxic compound in T lymphocytes, TrxR is required for its inactivation after it completes its defense role, further highlighting the importance of TrxR for post-immune functions.

Three TrxR isoforms, TrxR-1, TrxR-2, and TrxR-3, have been identified from mammals. TrxR-1 and TrxR-2 are localized to the cytosol and mitochondria, respectively, whereas TrxR-3 is exclusively expressed in the testis, where it acts as a thiol regulator (Urig and Becker, 2006). Mammalian TrxR proteins exhibit high sequence similarity to glutathione reductase, especially at the conserved Cys-Val-Asn-Val-Gly-Cys redox catalytic site. TrxR functions mostly relate to their basic role in Trx reduction by using NADH and NADPH, which are indirectly important in thioredoxin recycling (Mustacich and Powis, 2000). Thus, TrxR is apparently important in cell growth and apoptosis regulation, as well as in antioxidative defense in organisms. In addition, its function in the cellular environment is also important in recycling ascorbate by producing ascorbyl free radical, which is used as a marker of oxidative stress (Buettner and Jurkiewicz, 1993), in turn reducing the risk of triggering oxidative stress in cells.

TrxRs are widely distributed among eukaryotic and prokaryotic taxa; however, those found in prokaryotes and in some eukaryotes are rather different from mammalian TrxRs with respect to their molecular structure and substrate specificity. Low molecular weight TrxR variants (~35–37 kDa per monomer) are found commonly in Archaea, Bacteria, Fungi, and in some eukaryotes including plants and intracellular parasites (Brown et al., 1996; Bruchhaus and Tannich, 1995; Dai et al., 1996; Ellis et al., 1994), whereas high molecular weight variants (~55–56 kDa per monomer), which are analogous to glutathione reductases, are found prominently in mammals. However, to our knowledge, fish TrxR was exclusively reported from rainbow trout (*Oncorhynchus mykiss*) representing a teleost origin (Pacitti et al., 2014), in which two isoforms were identified and characterized.

The light of this background prompted us to characterize a teleostean TrxR ortholog (*RbTrxR-3*) from rock bream (*O. fasciatus*) at the molecular level, and compare the temporal transcriptional patterns of *RbTrxR-3* and its putative substrate, rock bream Trx-1 (*RbTrx-1*), under conditions of pathogenic stress. In addition, we investigated the functional properties of RbTrxR-3 that are important for its basic role in fish physiology, using its purified recombinant protein.

2. Materials and methods

2.1. Identification of complete RbTrxR-3 cDNA and genomic DNA sequences

A rock bream cDNA shotgun sequence database was established based on sequence data from a cDNA library constructed previously by using a next-generation sequencing technology, the GS-FLX titanium system (DNA Link, Rep. of Korea). A complete cDNA sequence with high sequence similarity to known TrxR-3 orthologs from other organisms was identified using NCBI BLAST. The complete *RbTrxR-3* genomic DNA (gDNA) sequence was obtained from a custom-constructed random-sheared BAC gDNA library (Lucigen®, USA). The library was screened to identify a putative BAC clone that contained *RbTrxR-3* by a polymerase chain reaction (PCR)-based approach using gene-specific primers: RbTrxR-3-qF and RbTrxR-3-qR (Table 1). *RbTrxR-3* was sequenced using the GS-FLX™ system (Macrogen, Korea).

Table 1
Primers used in this study.

Name	Purpose	Sequence (5′ → 3′)
RbTrxR-3_qF	BAC gDNA library screening and qPCR amplification of *RbTrxR-3*	AGGGTGGCACTGAGAGACAAGAA
RbTrxR-3_qR	BAC gDNA library screening and qPCR amplification of *RbTrxR-3*	AGGTCGTCACTGGTGATGCAGTA
RbTrx_qF	qPCR amplification of *RbTrx-1*	GGCTGGTGGTGGTGGACTT
RbTrx_qR	qPCR amplification of *RbTrx-1*	ACTCGGACACCTTCGCTTCATTCT
RbTrxR-3-F	Amplification of coding region (*Eco*R I)	GAGA GAgaattcATGCCTCCCATCGAAAGTGACAC
RbTrxR-3-R	Amplification of coding region (*Sal* I)	GAGA GAgtcgacTTAACCTCAGCAGCCGGCCTG
Rb-βF	qPCR amplification of rock bream β-actin gene	TCATCACCATCGGCAATGAGAGGT
Rb-βR	qPCR amplification of rock bream β-actin gene	TGATGCTGTTGTAGGTGGTCTCGT

2.2. RbTrxR-3 sequence profiles and phylogenetic analyses

The complete cDNA sequence and corresponding amino acid sequence of RbTrxR-3 were derived using DNAsist 2.2 software, and the putative TrxR domain architecture was predicted using ExPASy-prosite (http://prosite.expasy.org/), NCBI-CDS (http://www.ncbi.nlm.nih.gov/Structure/cdd/wrpsb.cgi), and SMART (http://smart.embl-heidelberg.de/) online servers. Putative SECIS elements were predicted using SECISearch online server (http://genome.unl.edu/SECISearch.html). Several important physicochemical properties of RbTrxR-3 were determined using the ExPASy ProtParam tool (http://web.expasy.org/protparam). The derived RbTrxR-3 sequence was compared with those of its homologs by performing pairwise sequence alignment and multiple-sequence alignment strategies, using EMBOSS Needle (http://www.Ebi.ac.uk/Tools/emboss/align) and ClustalW2 (http://www.Ebi.ac.uk/Tools/clustalw2) programs, respectively. The phylogenetic relationship of RbTrxR-3 with its vertebrate orthologs (including isoforms) was determined using MEGA software version 5 (Tamura et al., 2011), by the neighbor-joining method, supported by 1000 bootstrapped replicates. The exon–intron arrangement of the identified *RbTrxR-3* sequence was annotated using the NCBI-Spidey online server (http://www.ncbi.nlm.nih.gov/spidey) based on its complete cDNA sequence that has been identified previously.

2.3. Molecular cloning, over-expression, and purification of recombinant RbTrxR-3 (rRbTrxR-3)

The complete *RbTrxR-3* coding sequence was amplified by PCR using gene-specific cloning oligomers (Table 1) containing *Eco*RI and *Sal*I restriction sites. PCR amplification was performed in a TaKaRa thermal cycler (TaKaRa Korea Biomedical Inc., Korea) in a 50 μL reaction volume that contained 5 U of ExTaq polymerase (TaKaRa), 5 μL of 10× ExTaq buffer, and 4 μL of 2.5 mM dNTPs, 80 ng of DNA template, and 20 pmol of each oligomer. The following cycling conditions were used: an initial incubation at 94 °C for 3 min followed by 35 cycles of 94 °C for 30 s, 57 °C for 30 s, 72 °C for 2 min, and a final extension at 72 °C for 5 min. The resultant PCR product was ligated into pMAL-c2X vector, and the recombinant vector was transformed into *Escherichia coli* DH5α cells. The identity of the insert was confirmed by sequencing. Next, the recombinant vector was transformed into *E. coli* BL21 (DE3) cells, and selected putative transformants were grown overnight in 500 mL of Luria-Bertani broth, supplemented with 100 μg/mL of ampicillin and 0.5 mg/mL of glucose, at 37 °C with shaking (200 rpm). Once the OD_{600} of the culture reached 0.5, isopropyl-β-D-1-thiogalactopyranoside (IPTG) was added to a final concentration of 1 mM and the mixture was then incubated for 3 h at 37 °C to induce protein expression. Cells were subsequently chilled on ice for 30 min and harvested by cold centrifugation. The obtained pellets were resuspended in column buffer (20 mM Tris–HCl pH 7.4 and 200 mM NaCl) and stored at −20 °C overnight. Frozen cells were thawed on ice, lysed, and ruptured using cold sonication in the presence of lysozyme (1 mg/mL). The resultant whole cell lysate was centrifuged (9000 ×*g* for 30 min at 4 °C) and the supernatant (crude extract) was then purified to obtain rRbTrxR-3 by using the pMAL protein fusion and purification technique (New England Biolabs, USA). Finally, the concentration of the purified recombinant protein was determined using the Bradford method, and its integrity and purity were analyzed using 12% sodium dodecyl sulfate polyacrylamide gel electrophoresis (SDS-PAGE) under reducing as well as non-reducing conditions.

2.4. rRbTrxR-3 thiol reductase activity analysis

Reducing activity of rRbTrxR-3 against thiol groups in 5,5′-dithiobis(2-nitrobenzoic acid) (DTNB) was analyzed using a commercially available colorimetric assay kit (BioVision, USA) according to the manufacturer's instructions, with some minor modifications. Briefly, rRbTrxR-3 was diluted to different concentrations with the assay buffer (final volume of 50 μL) provided with the kit, and then combined with a reaction solution containing 30 μL of assay buffer, 8 μL of DTNB solution, and 2 μL of NADPH in 96-well microtiter plates. The samples were immediately incubated at 25 °C for 20 min, and the OD_{412} of each reaction was measured. The same procedure was performed using maltose-binding protein (MBP) and 50 μL of assay buffer in place of RbTrxR-3 as controls. OD_{412} values were calculated by subtracting the mean OD_{412} value of three replicates of the negative control (assay buffer) from that of each experimental sample.

2.5. Animal husbandry and tissue collection

Healthy rock breams, which were obtained from the Jeju Special Self-Governing Province Ocean and Fisheries Research Institute (Jeju, Republic of Korea), with an average body weight of 30 g were reared in a controlled environment (salinity 34 ± 1‰, pH 7.6 ± 0.5, and 22–24 °C). The animals were acclimatized for one week prior to experimentation. Within the acclimatization period, fish were fed with a commercially available fish feed. Whole blood (1 mL/fish) was collected from the caudal fin by using a sterilized syringe and the samples were centrifuged immediately at 3000 ×*g* for 10 min at 4 °C to separate the blood cells from the plasma. Collected cells were snap-frozen in liquid nitrogen. The gill, liver, skin, spleen, head kidney, muscle, brain, heart, kidney and intestine were excised from three animals and immediately snap-frozen in liquid nitrogen. Tissue samples were stored at −80 °C until total RNA was extracted.

2.6. Pathogen challenge experiments

To gain insights into the modulatory effects of common and potentially infectious pathogens on *RbTrxR-3* mRNA expression, two live bacterial pathogens, *Edwardsiella tarda* (*E. tarda*) and *Streptococcus iniae* (*S. iniae*) as well as a well-known fish viral pathogen, rock bream iridovirus (RBIV) were used to stimulate healthy rock breams, reared as described previously (Section 2.5), in a time-course immune challenge experiment. The complete experiment was performed as described in our previous report (Whang et al., 2011). Liver tissues of the experimental animals were collected as described in Section 2.5. At least three animals from each challenge group were sacrificed at each time point.

2.7. Total RNA extraction and cDNA synthesis

Total RNA was extracted from each of the tissues collected from healthy fish, as well as from the liver tissues from the immune-challenged group by using Tri Reagent™ (Sigma-Aldrich, USA) according to the vendor's protocol. The concentration of each extracted RNA sample was measured at 260 nm in a UV-spectrophotometer (Bio-Rad, USA) and diluted to 1 μg/μL. RNA (2.5 μg) from each tissue was used to synthesize cDNA by reverse transcription using a cDNA synthesis kit (TaKaRa, Japan) according to the manufacturer's instructions. Synthesized cDNAs were diluted 40-fold (total volume of 800 μL) and stored at −20 °C for future analysis.

2.8. Measurement of RbTrxR-3 and rock bream Trx-1 (RbTrx-1) mRNA expression levels in liver tissues by using quantitative PCR (qPCR)

RbTrxR-3 and *RbTrx-1* transcripts levels were measured in the liver tissues of infected fish as well as in the selected tissues of healthy fish (Section 2.5) by performing qPCR using the synthesized cDNAs as templates (Section 2.7). qPCR was perfomed using a Dice™ Real-time System (TP800; TaKaRa, Japan) Each 15 μL reaction contained 4 μL of diluted cDNA, 7.5 μL of 2× TaKaRa Ex Taq™, SYBR premix, 0.6 μL of each primer (RbTrxR-3_qF and RbTrxR-3_qR or RbTrx_qF and RbTrx_qR; Table 1), and 2.3 μL of ddH_2O, following essential MIQE

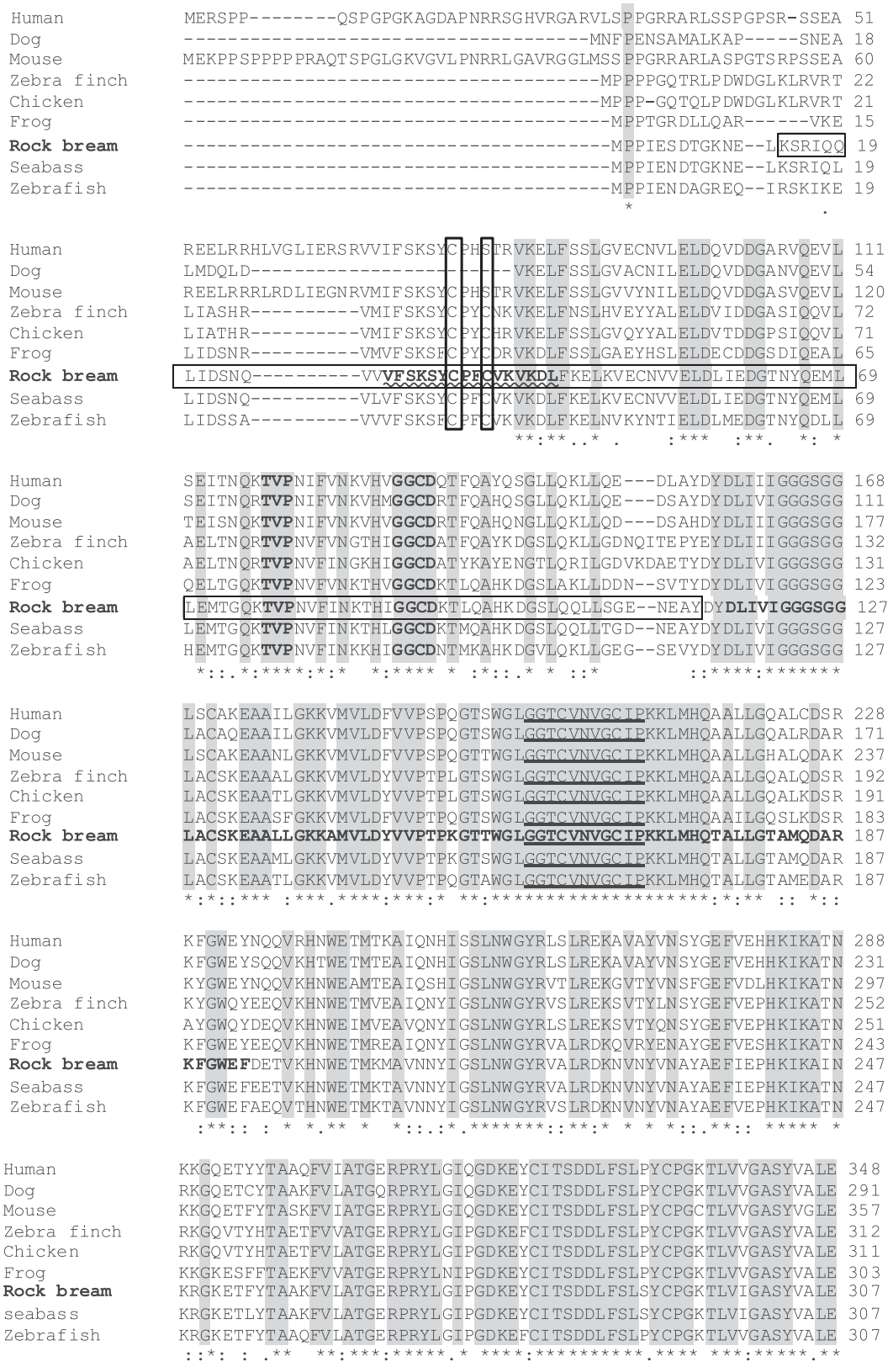

Fig. 1. Multiple-sequence alignment of RbTrxR-3 and its vertebrate orthologs. Sequence alignments were obtained using ClustalW server. Conserved residues are shaded in gray. The predicted glutaredoxin domain profile, glutaredoxin active site signature, and pyridine nucleotide-disulfide oxidoreductase class-I active site signature are indicated on the RbTrxR-3 sequence by a box, wavy underline, and normal underline, respectively. The putative FAD-binding signature is denoted in bold fonts and predicted pyridine nucleotide-disulfide oxidoreductase dimerization domain is represented by red colored letters. The selenocystein residues positioned at the 3′ of the sequences were denoted by 'U' and shaded in green color. Residues that form GSH-binding sites that are conserved in all the homologs are indicated by bold fonts (TVP and GGCD), and completely or partially conserved catalytic residues are indicated by vertical boxes.

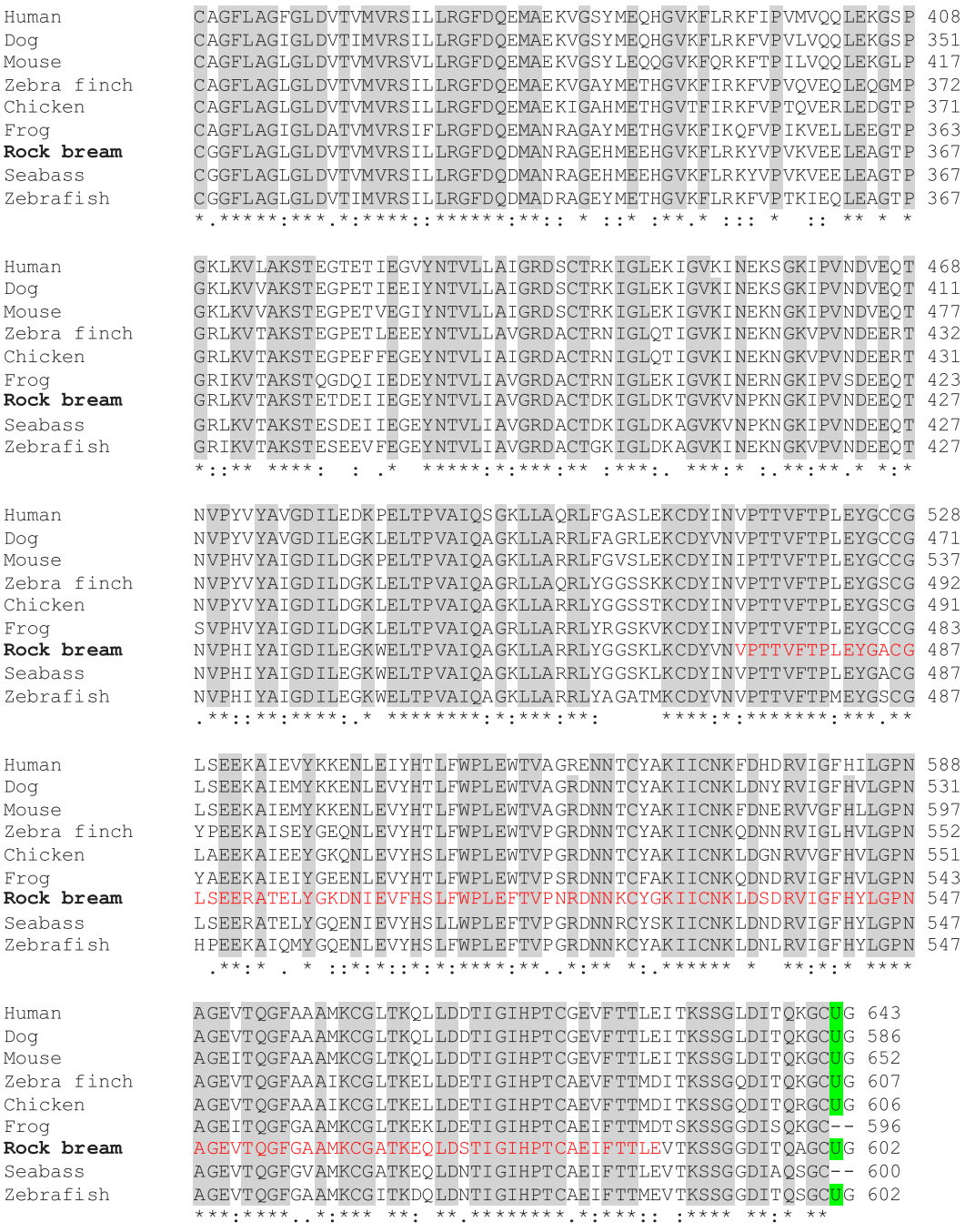

Fig. 1 (*continued*).

guidelines (Bustin et al., 2009). The full-length *RbTrx-1* coding sequence was obtained from the NCBI-GenBank database (accession no. AB603653) and used to design qPCR oligomers. The following qPCR conditions were used: an initial denaturation at 95 °C for 10 s; followed by 35 cycles of 95 °C for 5 s, 58 °C for 10 s, and 72 °C for 20 s; and a final cycle of 95 °C for 15 s, 60 °C for 30 s, and 95 °C for 15 s. The base line was set automatically by the Dice™ Real Time System software (version 2.00). *RbTrxR-3* mRNA expression levels were determined using the Livak ($2^{-\Delta\Delta CT}$) method (Livak and Schmittgen, 2001). The same qPCR cycling conditions were used to amplify the internal reference gene, rock bream β-actin (GenBank ID: FJ975146), using gene-specific primers (Table 1). All data are represented as the mean ± standard deviation (SD) of experiments performed in triplicate. Gene expression levels were compared to that of the rock bream β actin gene to obtain relative gene expression values at mRNA levels. The relative changes in *RbTrxR-3* and *RbTrx-1* expression at mRNA level were determined for the immune-challenged groups at various time points by normalizing the mRNA expression levels to those of the corresponding phosphate-buffered saline (PBS)-injected control, to eliminate the effect of the injection. Transcript levels in the uninjected control (0 h) were considered as baseline. The statistical difference between the experimental and uninjected control groups were analyzed using two tailed unpaired Student's *t*-tests. $P < 0.05$ was considered statistically significant.

Table 2
Percent similarity and identity values of RbTrxR-3 and its homologs.

Organism	Common Name	Protein	Accession number	Identity (%)	Similarity (%)	Length in amino acids
1. *Dicentrarchus labrax*	European seabass	Thioredoxin reductase 3	CBN80599	95.2	98.2	600
2. *Danio rerio*	Zebrafish	Thioredoxin reductase 3	NP898895	84.4	93.4	602
3. *Xenopus laevis*	African clawed frog	Thioredoxin reductase 3	NP001087660	75.8	89.0	596
4. *Taeniopygia guttata*	Zebra finch	Thioredoxin reductase 3	NP001245307	72.9	85.5	607
5. *Gallus gallus*	Chicken	Thioredoxin reductase 3	NP001116249	72.5	84.6	606
6. *Canis lupus familiaris*	Dog	Thioredoxin reductase 3	NP001116250	70.5	83.1	586
7. *Pteropus alecto*	Black flying fox	Thioredoxin reductase 3	ELK13077	68.1	81.2	636
8. *Myotis brandtii*	Bat	Thioredoxin reductase 3	EPQ08225	66.2	79.6	647
9. *Mus musculus*	Mouse	Thioredoxin reductase 3	NP001171529	64.5	78.0	652
10. *Homo sapiens*	Human	Thioredoxin reductase 1	NP001087240	64.5	77.0	649
11. *Xenopus tropicalis*	Western clawed frog	Thioredoxin reductase 1	NP001243400	62.1	74.1	653
12. *Mus musculus*	Mouse	Thioredoxin reductase 1	NP001035978	61.4	71.8	499
13. *Homo sapiens*	Human	Thioredoxin reductase 3	NP443115	55.0	66.5	643
14. *Homo sapiens*	Human	Thioredoxin reductase 2	NP006431	45.5	59.3	524
15. *Mus musculus*	Mouse	Thioredoxin reductase 2	NP038739	44.6	57.9	527

3. Results and discussion

3.1. Molecular properties and sequence similarity of RbTrxR-3

The full-length cDNA sequence of *RbTrxR-3* comprised 3247 nucleotides, consisting of an 1806-bp open reading frame (ORF) as well as 5′ and 3′ untranslated regions (UTRs) that were 256 bp and 1182 bp, respectively. As expected, we could identify an in-frame opal codon (^{1798}TGA^{1800}) in *RbTrxR-3* ORF which probably codes for a selenocysteine amino acid (U in Fig. 1), positioned one amino acid before the termination codon of RbTrxR-3, confirming the characteristic feature of selenoproteins, including thioredoxin reductases. Moreover, we could decipher the loose SECIS element pattern in 3′ UTR (^{2450}GTGAC^{2455}, ^{2468}AA^{2469} and ^{2497}CGAT^{2500}) which is known to direct the insertion mechanism of selenocystein residue at the position of TGA codon, using SECISearch server, based on non-canonical A-G pairs of human TrxR-3 (Hatfield and Gladyshev, 2002). This evidence further validates that the aforementioned opal codon likely encodes a U residue in RbTrxR-3. Based on our *in silico* analysis, we determined that the identified ORF encoded a 602-amino acid protein with a molecular mass of ~66 kDa and theoretical isoelectric point of 5.8. Protein and cDNA sequence information for RbTrxR-3 was deposited in the NCBI-GenBank database under the accession number KF742679. Our computational domain analysis showed that RbTrxR-3 possesses typical TrxR features including a proximal glutaredoxin domain (residues 14–114), glutaredoxin active site (residues 28–43), pyridine nucleotide-disulfide oxidoreductase class-1 active site (PYRIDINE REDOX_1; residues 159–169), putative FAD-binding domain (residues 117–193), and pyridine nucleotide-disulfide oxidoreductase dimerization domain (residues 473–586) (Fig. 1). Multiple-sequence alignments showed that cysteine residues in the RbTrxR-3 active site (residues 34 and 37) were completely or partially conserved, while the PYRIDINE REDOX_1 site was conserved in all sequences examined. The predicted glutathione binding sites in RbTrxR-3 (residues 77, 78, 79, 89, 90, 91, and 92) also showed good conservation. Pairwise sequence alignments of RbTrxR-3 and its orthologs confirmed that it was a TrxR homolog, sharing prominent percent identity and similarity values to other teleostean TrxRs, especially to that of *Dicentrarchus labrax* (Table 2).

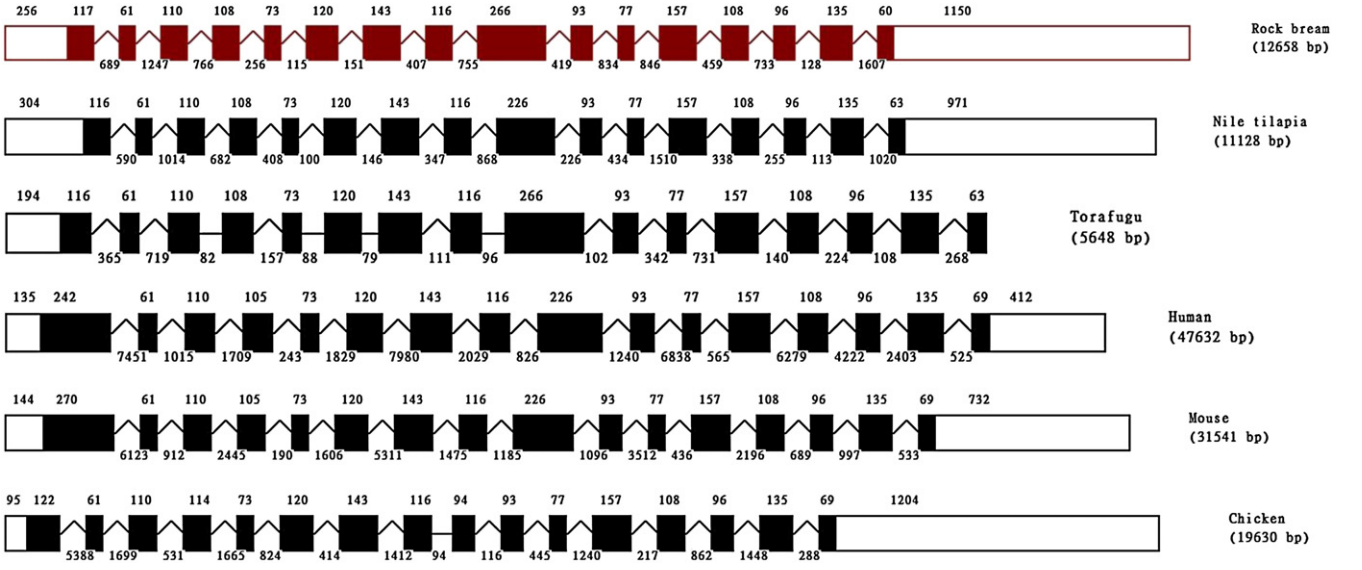

Fig. 2. Genomic architecture of *RbTrxR-3* and its vertebrate orthologs. UTR and coding regions are represented by empty and filled boxes, respectively. Introns less than 100 bp are denoted using black lines and those >100 bp are depicted as Λ-shaped lines. The intron and exon lengths are indicated at the top and bottom of each structure, respectively. The genomic DNA sequence information for each ortholog was obtained from the NCBI-GenBank database: Nile tilapia, 100702976; torafugu, 101068545; mouse, 232223; human, 114112; and chicken, 416031.

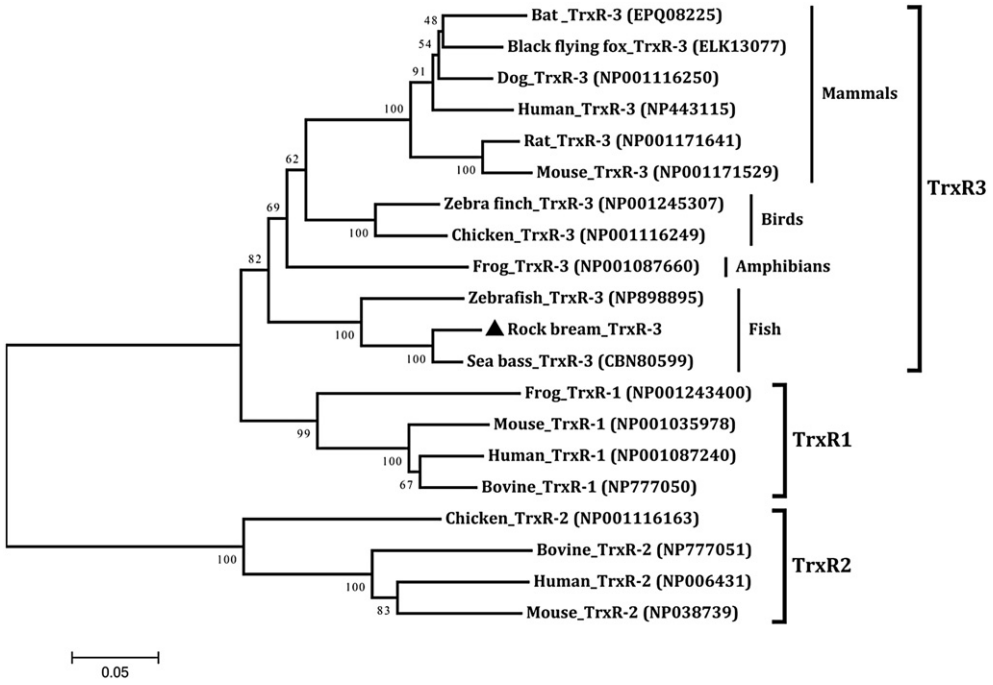

Fig. 3. Phylogenetic reconstruction of RbTrxR-3. The evolutionary development of RbTrxR-3 was analyzed with its different homologs (including the isoforms of TrxRs) categorized under different taxonomic groups based on the multiple alignment profile of the protein sequences generated by the neighbor-joining method using MEGA 5.0 software. Bootstrap support values corresponding to each branch are indicated. The NCBI-GenBank accession numbers of each TrxR ortholog are listed in Table 2.

3.2. Comparative analysis of RbTrxR-3 gene architecture

Using the Spidey server, we determined that *RbTrxR-3* consists of 16 exons and 15 introns spread along a 12658 bp sequence, according to the canonical AG-GT splicing rule (Fig. 2). To gain a better understanding of the molecular evolution and genomic diversity of TrxR-3, we compared the gDNA sequences TrxR-3 genes from a number of vertebrate taxa (Fig. 2). With the exception of the lengths of exons 4 and 9, the architecture of the internal exons—those flanked by the first and last exons were conserved among the different taxonomic groups, which included teleosts, mammals, and birds. Interestingly, the size of each exon was found to be conserved among teleosts; further teleosts and mammals shared 13 exons with equal length (exon 2 to 15, except exon 4). Notably, the number of exons (16) in lower vertebrates (*i.e.*, teleosts) and higher vertebrates (*i.e.*, mammals and birds) were highly conserved, confirming that no gain or loss of introns had occurred during the molecular evolution of vertebrate TrxR-3 s. Moreover, the splitting of the *TrxR-3* into a relatively high number of exons could indicate the existence of *TrxR-3* splice variants in teleosts and other vertebrates (Keren et al., 2010) and tightly regulated gene expression, a process in which introns are known to be involved (Rose, 2008). However, these predictions warrant further investigation. The overall comparison of *TrxR-3* gene architecture in vertebrates suggests that the gene has a slow rate in genomic evolution and a greater potency of eliciting significant diversity at protein level through formation of spliced variants.

3.3. Phylogenetic reconstruction of RbTrxR-3

As expected, our phylogenetic reconstruction clearly separated the different vertebrate TrxR orthologs into three main clusters according to the basic isoforms: TrxR-1, TrxR-2, and TrxR-3. Within the TrxR-3 cluster, mammalian, bird, amphibian, and fish orthologs clustered closely and independently, in which RbTrxR-3 clustered within the fish (piscine) clade (Fig. 3). RbTrxR-3 subclustered with sea bass TrxR-3 within the fish clade, with a supporting bootstrap value of 100. However, zebrafish TrxR-3 showed a relatively distant evolutionary relationship with the other two marine teleost homologs. Taken together, our phylogenetic analysis, based on the TrxR protein sequences of different species, confirmed that RbTrxR-3 is a vertebrate TrxR-3 isoform that has evolved from a common ancestral piscine gene.

3.4. Integrity of purified rRbTrxR-3

We performed SDS-PAGE analysis on samples collected at different steps in the overexpression and purification procedure of rRbTrxR-3. The recombinant RbTrxR-3-MBP fusion protein was successfully

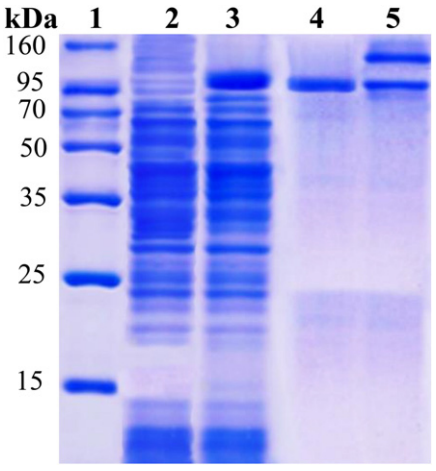

Fig. 4. SDS-PAGE analysis of the rRbTrxR-3 fusion protein at different steps in the overexpression and purification process. Lane 1, protein size marker (Enzynomics, Korea); lane 2, total cellular extract from *Escherichia coli* BL21 (DE3) carrying the rRbTrxR-3-MBP expression vector prior to the IPTG induction; lane 3, crude rRbTrxR-3 fusion protein extract; lane 4, purified recombinant fusion protein (rRbTrxR-33-MBP) under reducing conditions; and lane 5, purified recombinant fusion protein (rRbTrxR-3-MBP) under non-reducing conditions.

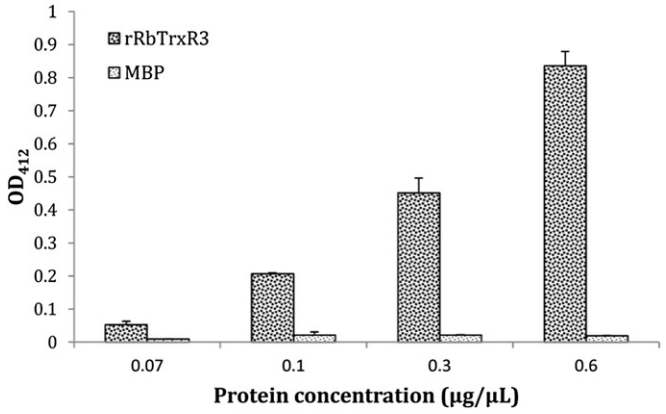

Fig. 5. *In vitro* DTNB-reducing activity of rRbTrxR-3. Reducing activities of rRbTrxR-3 and MBP towards DTNB were measured using a colorimetric assay. The yellow-colored reduction product produced in each sample was quantified using OD_{412} measurements. Error bars represent SD (n = 3).

expressed in *E. coli* BL21 cells and purified (Fig. 4). A single band (Fig. 4, lane 2) was observed at ~102.5 kDa, consistent with predicted molecular mass of reduced RbTrxR-3 (~66 kDa; mass of MBP is ~42.5 kDa), confirming the purity and integrity of the recombinant protein. Interestingly, two bands were resolved for the eluted fusion protein when the polyacrylamide gel was run under non-reducing conditions (Fig. 4, lane 5) suggesting that rRbTrxR-3 formed homodimers. Because homodimerization is a characteristic of TrxRs, these data further support our prediction on rRbTrxR-3's homology to known TrxR-3s.

3.5. Thiol-reductase activity of RbTrxR-3

In the presence of NADPH, rRbTrxR-3 reduced the thiol groups of DTNB, producing 5′-thiol-2-nitrobenzoic acid (TNB^{2-}), which generates a strong yellow color with an absorption maximum (λ_{max}) of 412 nm (Fig. 5). OD_{412} values increased with increasing rRbTrxR-3 concentration. Thus, RbTrxR-3 possesses a typical functional property of TrxR family members, suggesting their functional homology. Compared to rRbTrxR-3, MBP had negligible reducing activity against DTNB, as indicated by significantly lower OD_{412} values, suggesting that MBP did not affect the function of the rRbTrxR-3 fusion protein. Consistent with the dose-dependent thiol-reducing activity of RbTrxR-3 observed in this study, *Entamoeba histolytica* (Arias et al., 2012) and *Caenorhabditis elegans* (Lacey and Hondal, 2006) TrxR proteins also demonstrated marked concentration- and NADPH-dependent thiol reductase activities against DTNB.

3.6. Distribution of RbTrxR-3 mRNA in rock bream tissues

RbTrxR-3 was ubiquitously distributed in rock bream tissues, with blood tissue showing the highest mRNA expression level (Fig. 5). Gill and liver tissues had moderately high *RbTrxR-3* transcript levels. The differential levels of *RbTrxR-3* mRNA expression detected in the different tissue types examined may reflect distinct levels of metabolic activity in those tissues, which may in turn reflect differences in the ROS levels in tissues, because TrxR has a known function in balancing ROS levels. Blood cells, especially phagocytic cells, can produce excessive amounts of ROS in response to invading pathogens as a first-line host defense mechanism, eventually activating immune signaling pathways (Kohchi et al., 2009). Moreover, blood cells have a higher level of oxygen consumption, which in turn potentiates ROS formation. Therefore, we speculate that TrxRs are expressed at high levels in certain tissues, such as in rock bream blood cells, to maintain an optimum redox balance. TrxR can also directly act upon NK-lysin-like cytotoxic compounds produced by T-lymphocytes to deactivate them after they have completed their function (Andersson et al., 1996). This may also explain the pronounced *RbTrxR-3* mRNA expression in blood cells. Similarly, one isoform of rainbow trout TrxR-3 (TrxR-3a) showed its highest basal expression in blood cells whereas the other (TrxR-3b) was also found to be pronouncedly expressed in blood (Pacitti et al., 2014). The gills of fish are continuously exposed to the aquatic environment,

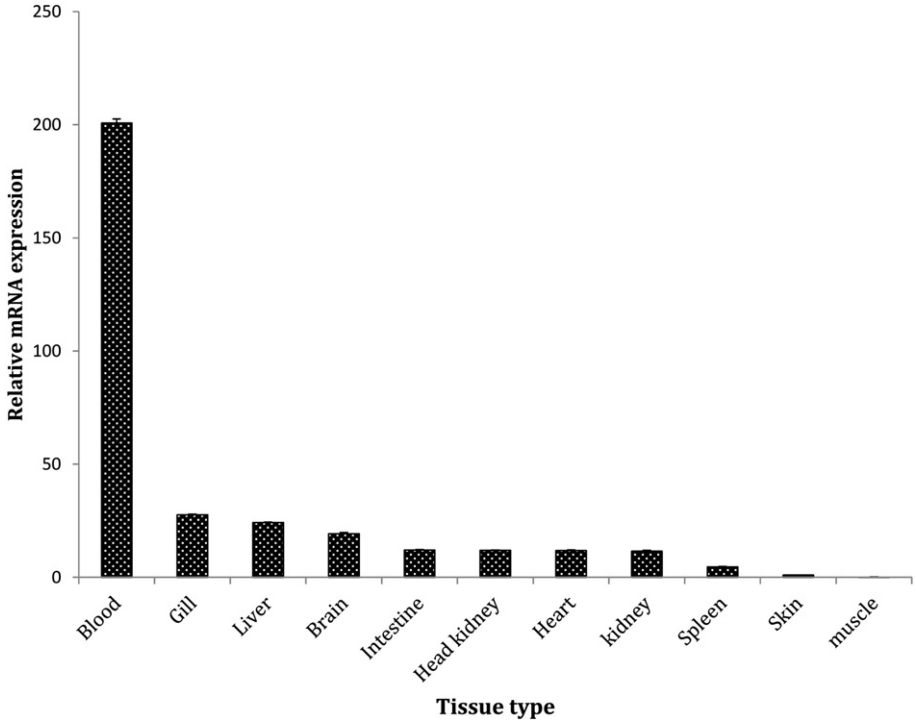

Fig. 6. Tissue distribution of *RbTrxR-3* mRNA expression, analyzed using qPCR. Relative expression values were determined by comparing the expression in each tissue to that in the skin. Error bars represent SD (n = 3).

increasing the risk of frequent microbial infections. As mentioned above, ROS are formed in response to invading pathogenic microorganisms as a primitive immune defense strategy that is executed by immune cells in tissues including the gills (Kohchi et al., 2009). Therefore, to prevent harmful effects of oxidative stress on these cells, antioxidative defense mechanisms must be activated in host organisms, in which the thioredoxin system plays an indispensable role. Therefore, pronounced TrxR expression would be expected in gill tissues of teleost fish, consistent with our findings. Moreover, the high levels of *RbTrxR-3* in liver tissues can be attributed to the prominent metabolic activity of liver cells, which contributes to ROS production (Martin et al., 2002). In response to oxidative stress, liver cells can undergo apoptosis (Kamata et al., 2005); thus, the abundant mRNA expression of *RbTrxR-3* in liver tissues may relate to the known anti-apoptotic function of TrxRs. Although, pronounced expression of other fish TrxRs in the liver have not been reported to date, it is not uncommon to find abundant TrxR expression in the livers of higher vertebrates such as rats (Lee et al., 1999).

3.7. Temporal transcriptional response of RbTrxR-3 to live pathogenic stimuli

Liver tissues are known to play an important role in host immunity (Sheth and Bankey, 2001); thus, we examined the transcriptional response of *RbTrxR-3* in the livers of rock breams exposed to live bacterial and viral pathogenic stimuli. Moreover, in parallel, we investigated the transcriptional responses of the putative substrate *RbTrx-1* to the same stimuli, in order to compare those with corresponding expressional modulation of *RbTrxR-3*, deciphering the expressional behavior of the thioredoxin system under pathogen stress. Both stimuli significantly increased *RbTrxR-3* mRNA expression ($P < 0.05$) during the middle (6 h and 12 h post-injection [p.i.]) and late phases (48 h p.i.) of the experimental period (Fig. 6A). Interestingly, transcript levels of the putative RbTrxR-3 substrate in rock breams, *RbTrx-1*, were also elevated significantly ($P < 0.05$) during the middle (12 h p.i.) and late phase (24 h, and 48 h p.i.) in response to the live pathogens RBIV and *E. tarda*, while live *S. iniae* treatment was inducing its basal transcription throughout the whole period of post immune challenge (Fig. 7). In contrast, *RbTrx-1* transcript levels were found to be significantly ($P < 0.05$) down-regulated at 6 h p.i. following RBIV challenge (Fig. 6B). Some viruses are known to diminish the expression of antioxidant enzymes to induce ROS formation in host cells in order to induce apoptosis and spread the infection to the uninfected cell population (Borjesson et al., 2005; Yang et al., 2010). Thus, the initial down-regulation of *RbTrx-1* transcript may be part of the mechanism of RBIV infection.

Phagocytosis, a process associated with the innate immune system, can efficiently mediate the recognition and elimination of pathogenic invaders (Vatansever et al., 2013). In this complex process, phagocytic cells, such as macrophages and neutrophils in different immune defense-related tissues including the liver engulf invading microbial pathogens and destroy them using numerous chemical species, including ROS. Therefore, immediately after microbial infection, ROS production is expected to increase, leading to oxidative burst (Forman and Torres, 2001). As a consequence, endogenous antioxidative defense mechanisms (Nordberg and Arner, 2001) are activated to counterbalance the ROS surplus. In this regard, it is not unexpected to observe the activation of Trx system, especially in liver cells. Thus, the marked increase we observed in *RbTrxR-3* expression at mRNA level most likely to be occurred in response to live pathogenic stress. Consistent with these findings, *RbTrx-1* transcript levels were elevated in response to the same stimuli. The reduced form of Trx, which is produced as a result of TrxR catalytic activity, was found to activate several transcriptional factors, including NF-κB (Nishiyama et al., 2001), that are known to induce the expression of cytokines and antimicrobial effectors (Hayden et al., 2006). Moreover, TrxRs can act upon antimicrobial compounds such as NK-lysin to inactivate them upon completion of their antimicrobial function (Andersson et al., 1996). These facts may also explain the elevated levels of *RbTrxR-3* transcript in liver tissue in rock breams exposed to live bacterial and viral stimuli.

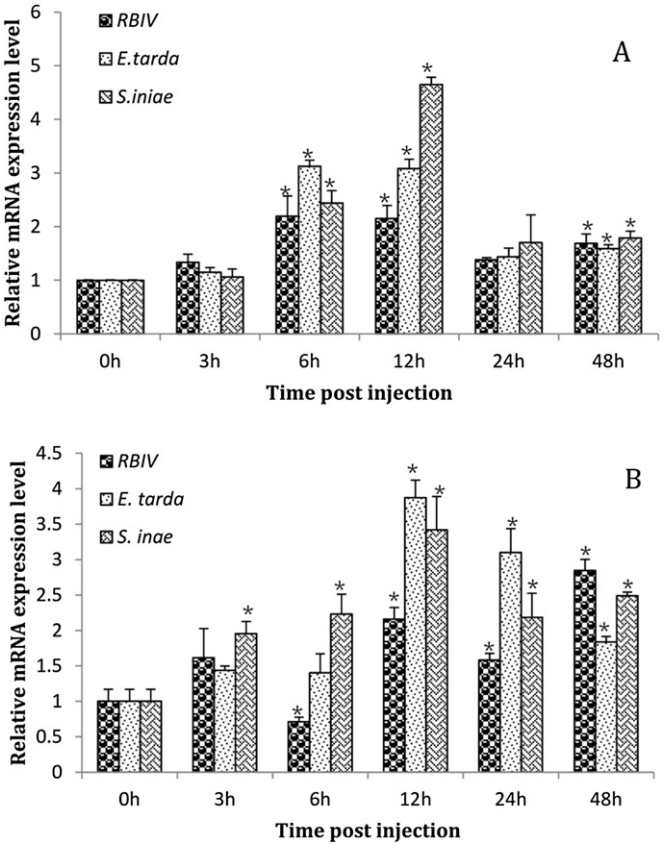

Fig. 7. Temporal mRNA expression of *RbTrxR-3* (A) and *RbTrx-1* (B) in the liver tissues of rock breams, under live pathogen stress induced by *Edwardsiella tarda*, *Streptococcus iniae*, and RBIV. The relative expression levels were calculated using the $2^{-\Delta\Delta CT}$ method, using rock bream β-actin as a reference gene. Expression levels were further normalized to the corresponding expression levels in PBS-injected controls at each time point. The relative expression at 0 h post-stimulation (uninjected control) was set as the baseline. Error bars represents SD (n = 3); *$P < 0.05$.

4. Conclusion

Here, we characterized a rock bream TrxR and investigated its transcriptional response to the pathogen invasion, along with functional properties that are important in host antioxidant defense. The results of our *in silico* homology analysis and phylogenetic construction showed that RbTrxR-3 is a TrxR family ortholog. The genomic architecture of *RbTrxR-3* suggests its potency to be contributed in diversity at protein level, probably forming its spliced variants. Moreover, the ubiquitous mRNA expression of this TrxR ortholog highlights its putative functional importance in fish physiology. Interestingly, the transcriptional response of *RbTrxR-3* in the livers of rock breams under live pathogen stress correlated with the temporal mRNA expression pattern of its putative substrate, *RbTrx-1*, suggesting that it may play an important role in immune or post-immune responses. In addition, the detectable thiol reductase activity of RbTrxR-3 further hints its plausible involvement in the rock bream Trx system. Overall, the findings of this study indicate that RbTrxR-3 plausibly plays a role in defending against oxidative stress.

Acknowledgments

This research was a part of the project titled 'Fish Vaccine Research Center', funded by the Ministry of Oceans and Fisheries, Korea.

References

Andersson, M., Holmgren, A., Spyrou, G., 1996. NK-lysin, a disulfide-containing effector peptide of T-lymphocytes, is reduced and inactivated by human thioredoxin reductase. J. Biol. Chem. 271, 10116–10120. http://dx.doi.org/10.1074/jbc.271.17.10116.

Arias, D.G., Regner, E.L., Iglesias, A.A., Guerrero, S.A., 2012. *Entamoeba histolytica* thioredoxin reductase: molecular and functional characterization of its atypical properties. Biochim. Biophys. Acta 1820, 1859–1866. http://dx.doi.org/10.1016/j.bbagen.2012.08.020.

Baker, A., Payne, C.M., Briehl, M.M., Briehi, M.M., Powis, G., 1997. Thioredoxin, a gene found overexpressed in human cancer, inhibits apoptosis in vitro and in vivo. Cancer Res. 57, 5162–5167.

Bjornstedt, M., Hamberg, M., Kumar, S., Xue, J., Holmgren, A., 1995. Human thioredoxin reductase directly reduces lipid hydroperoxides by NADPH and Selenocysteine strongly stimulates the reaction via catalytically generated selenols. J. Biol. Chem. 270, 11761–11764.

Borjesson, D.L., Kobayashi, S.D., Whitney, A.R., Voyich, J.M., Argue, C.M., Deleo, F.R., 2005. Insights into pathogen immune evasion mechanisms: *Anaplasma phagocytophilum* fails to induce an apoptosis differentiation program in human neutrophils. J. Immunol. 174, 6364–6372.

Brown, M., Upcroft, A., Upcroft, P., 1996. A thioredoxin reductase-class of disulphide reductase in the Protozoan parasite *Giardia duodenalis*. Mol. Biochem. Parasitol. 83, 211–220.

Bruchhaus, I., Tannich, E., 1995. Identification of an *Entamoeba histolytica* gene encoding a protein homologous to prokaryotic disulphide oxidoreductases. Mol. Biochem. Parasitol. 70, 187–191.

Buettner, G.R., Jurkiewicz, B.A., 1993. Ascorbate free radical as a marker of oxidative stress: an EPR study. Free Radic. Biol. Med. 14, 49–55.

Bustin, S.A., Benes, V., Garson, J.A., Hellemans, J., Huggett, J., Kubista, M., Mueller, R., Nolan, T., Pfaffl, M.W., Shipley, G.L., Vandesompele, J., Wittwer, C.T., 2009. The MIQE guidelines: minimum information for publication of quantitative real-time PCR experiments. Clin. Chem. 55, 611–622. http://dx.doi.org/10.1373/clinchem.2008.112797.

Casso, D., Beach, D., 1996. A mutation in a thioredoxin reductase homolog suppresses p53-induced growth inhibition in the fission yeast *Schizosaccharomyces pombe*. Mol. Gen. Genet. 252, 518–529.

Chae, H.Z., Chung, S.J., Rhee, S.G., 1994. Thioredoxin-dependent peroxide reductase from yeast. J. Biol. Chem. 269, 27670–27678.

Dai, S., Saarinen, M., Ramaswamy, S., Meyer, Y., Jacquot, J.P., Eklund, H., 1996. Crystal structure of *Arabidopsis thaliana* NADPH dependent thioredoxin reductase at 2.5 A resolution. J. Mol. Biol. 264, 1044–1057. http://dx.doi.org/10.1006/jmbi.1996.0695.

Ellis, J.E., Yarlett, N., Cole, D., Humphreys, M.J., Lloyd, D., 1994. Antioxidant defences in the microaerophilic protozoan *Trichomonas vaginalis*: comparison of metronidazole-resistant and sensitive strains. Microbiology 140 (Pt 9), 2489–2494.

Forman, H.J., Torres, M., 2001. Signaling by the respiratory burst in macrophages. IUBMB Life 51, 365–371. http://dx.doi.org/10.1080/15216540152846122.

Gasdaska, J.R., Powis, G., 1995. Cell growth stimulation by the redox occurs by a novel helper mechanism thioredoxin. Cell Growth Differ. 6, 1643–1650.

Hatfield, D.L., Gladyshev, V.N., 2002. How selenium has altered our understanding of the genetic code. Mol. Cell. Biol. 22, 3565–3567.

Hayden, M.S., West, A.P., Ghosh, S., 2006. NF-kappaB and the immune response. Oncogene 25, 6758–6780. http://dx.doi.org/10.1038/sj.onc.1209943.

Holmgren, A., 1979. Reduction of disulfides by thioredoxin. Exceptional reactivity of insulin and suggested functions of thioredoxin in mechanism of hormone action. J. Biol. Chem. 254.

Kamata, H., Honda, S.-I., Maeda, S., Chang, L., Hirata, H., Karin, M., 2005. Reactive oxygen species promote TNFalpha-induced death and sustained JNK activation by inhibiting MAP kinase phosphatases. Cell 120, 649–661. http://dx.doi.org/10.1016/j.cell.2004.12.041.

Keren, H., Lev-Maor, G., Ast, G., 2010. Alternative splicing and evolution: diversification, exon definition and function. Nat. Rev. Genet. 11, 345–355.

Kohchi, C., Inagawa, H., Nishizawa, T., Soma, G.-I., 2009. ROS and innate immunity. Anticancer Res. 29, 817–822.

Lacey, B.M., Hondal, R.J., 2006. Characterization of mitochondrial thioredoxin reductase from *C. elegans*. Biochem. Biophys. Res. Commun. 346, 629–636. http://dx.doi.org/10.1016/j.bbrc.2006.05.095.

Laurent, T.C., Moore, E.C., Reichard, P., 2013. Enzymatic synthesis of and characterization of thioredoxin, the hydrogen synthesis of deoxyribonucleotides. J. Biol. Chem. 239, 3439–3444.

Lee, S. Rock, Kim, J.R., Kwon, K.S., Yoon, H.W., Levine, R.L., Ginsburg, A., Rhee, S.U., 1999. Molecular cloning and characterization of a mitochondrial selenocysteine-containing thioredoxin reductase from rat liver. J. Biol. Chem. 274, 4722–4734. http://dx.doi.org/10.1074/jbc.274.8.4722.

Livak, K.J., Schmittgen, T.D., 2001. Analysis of relative gene expression data using real-time quantitative PCR and the 2(−Delta Delta C(T)) Method. Methods 25, 402–408. http://dx.doi.org/10.1006/meth.2001.1262.

Lu, J., Holmgren, A., 2012. Thioredoxin system in cell death progression. Antioxid. Redox Signal. 17, 1738–1747.

Martin, R., Fitzl, G., Mozet, C., Martin, H., Welt, K., Wieland, E., 2002. Effect of age and hypoxia/reoxygenation on mRNA expression of antioxidative enzymes in rat liver and kidneys. Exp. Gerontol. 37, 1479–1485.

May, J.M., Mendiratta, S., Hill, K.E., Burk, R.F., 1997. Reduction of dehydroascorbate to ascorbate by the selenoenzyme thioredoxin reductase. J. Biol. Chem. 272, 22607–22610. http://dx.doi.org/10.1074/jbc.272.36.22607.

May, J.M., Cobb, C.E., Mendiratta, S., Hill, K.E., Burk, R.F., 1998. Reduction of the ascorbyl free radical to ascorbate by thioredoxin reductase. J. Biol. Chem. 273, 23039–23045. http://dx.doi.org/10.1074/jbc.273.36.23039.

Mohapatra, S., Chakraborty, T., Kumar, V., DeBoeck, G., Mohanta, K.N., 2013. Aquaculture and stress management: a review of probiotic intervention. J. Anim. Physiol. Anim. Nutr. (Berl.) 97, 405–430. http://dx.doi.org/10.1111/j.1439-0396.2012.01301.x.

Mustacich, D., Powis, G., 2000. Thioredoxin reductase. Biochem. J. 346 (Pt 1), 1–8.

Nishiyama, A., Masutani, H., Nakamura, H., Nishinaka, Y., Yodoi, J., 2001. Redox regulation by thioredoxin and thioredoxin-binding proteins. IUBMB Life 52, 29–33. http://dx.doi.org/10.1080/15216540252774739.

Nordberg, J., Arner, E.S.J., 2001. Reactive oxygen species, antioxidants, and the mammalian thioredoxin system. Free Radic. Biol. Med. 31, 1287–1312.

Nordberg, J., Holmgren, A., Arne, E.S.J., 1996. Efficient reduction of lipoamide and lipoic acid by mammalian thioredoxin reductase. Biochem. Biophys. Res. Commun. 225, 268–274.

Pacitti, D., Wang, T., Martin, S.A.M., Secombes, C.J., Sweetman, J., 2014. Insights into the fish thioredoxin system: expression profile of thioredoxin and thioredoxin reductase in rainbow trout (*Oncorhynchus mykiss*) during infection and in vitro stimulation. Dev. Comp. Immunol. 42, 261–277.

Rose, A.B., 2008. Intron-mediated regulation of gene expression. Curr. Top. Microbiol. Immunol. 326, 277–290.

Sheth, K., Bankey, P., 2001. The liver as an immune organ. Curr. Opin. Crit. Care 7, 99–104.

Tamura, K., Peterson, D., Peterson, N., Stecher, G., Nei, M., Kumar, S., 2011. MEGA5: molecular evolutionary genetics analysis using maximum likelihood, evolutionary distance, and maximum parsimony methods. Mol. Biol. Evol. 28, 2731–2739.

Urig, S., Becker, K., 2006. On the potential of thioredoxin reductase inhibitors for cancer therapy. Semin. Cancer Biol. 16, 452–465. http://dx.doi.org/10.1016/j.semcancer.2006.09.004.

Vatansever, F., de Melo, W.C.M.A., Avci, P., Vecchio, D., Sadasivam, M., Gupta, A., Chandran, R., Karimi, M., Parizotto, N.A., Yin, R., Tegos, G.P., Hamblin, M.R., 2013. Antimicrobial strategies centered around reactive oxygen species — bactericidal antibiotics, photodynamic therapy, and beyond. FEMS Microbiol. Rev. 37, 955–989. http://dx.doi.org/10.1111/1574-6976.12026.

Whang, I., Lee, Y., Lee, S., Oh, M.-J., Jung, S.-J., Choi, C.Y., Lee, W.S., Kim, H.S., Kim, S.-J., Lee, J., 2011. Characterization and expression analysis of a goose-type lysozyme from the rock bream Oplegnathus fasciatus, and antimicrobial activity of its recombinant protein. Fish Shellfish Immunol. 30, 532–542. http://dx.doi.org/10.1016/j.fsi.2010.11.025.

Yang, T.C., Lai, C.C., Shiu, S.L., Chuang, P.H., Tzou, B.C., Lin, Y.Y., Tsai, F.J., Lin, C.W., 2010. Japanese encephalitis virus down-regulates thioredoxin and induces ROS-mediated ASK1-ERK/p38 MAPK activation in human promonocyte cells. Microbes Infect. 12, 643–651.